World Conference on
Timber Engineering
Oslo 2023

MODELLING SEISMIC ISOLATION BEARING FOR WOOD BUILDINGS

Asif Iqbal[1], Angelo Aloisio[2] and Massimo Fragiacomo[3]

ABSTRACT: This paper discusses the details of modelling a type of seismic isolator, named RoGlider, suitable for wood buildings. An analytical model of the bearing and estimate the parameters of a classical Bouc-Wen model representative of this device is presented. RoGlider is found to be useful for seismic protection and the proposed model can represent the isolation system with sufficient accuracy.

KEYWORDS: Seismic Isolation, Bouc-Wen Model, Wood Buildings

1. INTRODUCTION

The RoGlider, shown in Figure 1, is a sliding bearing which includes an elastic restoring force [1,2]. The actual configuration is dependent on the details of the structure being isolated and the expected earthquake. It consists of two flat steel plates with a puck between the plates. The puck consists of alternating layers of rubber and sheet steel, similar to the arrangement used in elastomeric bearings and Lead Rubber Bearings. The sliding elements such as PTFE are mounted at the ends of the puck. The two rubber membranes are attached to the puck with each being joined to either the top or the bottom plates thereby making a sealed unit. When the top and bottom plates slide sideways with respect to each other diagonally opposing parts of the membrane undergo tension or compression. The tension components provide the restoring force between the plates.

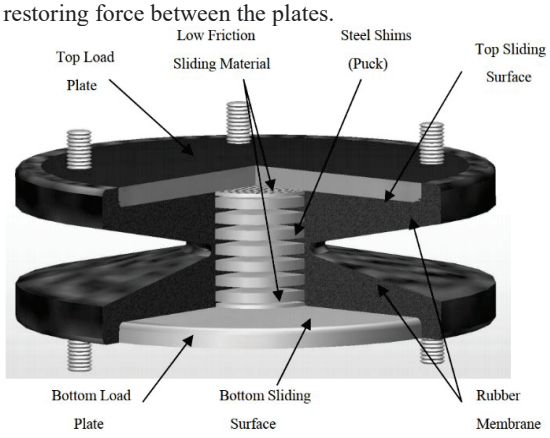

Figure 1: *Sectional view of RoGlider.*

With the special arrangement (Figure 3) and geometry (Figure 4), RoGlider is characterized by a lower lateral stiffness compared to classical elastomeric isolators. This feature enables the RoGlider to be used for isolating lightweight structures. The lower lateral stiffness guarantees the attainment of higher natural periods of vibration. Figure 2 shows a typical hysteresis plot.

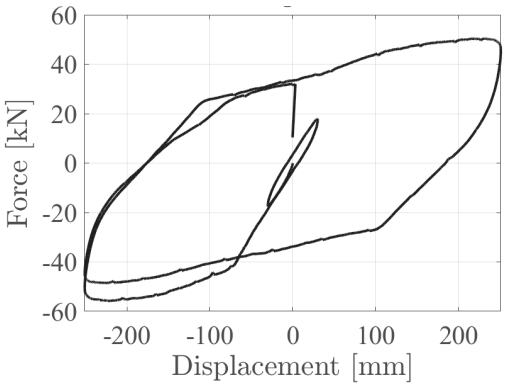

Figure 2*: Hysteresis of RoGlider*

2. ROGLIDER PROPERTIES

RoGlider bearings went through extensive testing by the developers and also during a research project at BRANZ in New Zealand [3]. Robinson et al. tested the bearing at their facility (Figure 4) under a range of vertical loads and displacement range [1]. It is visible that the bearings can carry significant vertical load at design-level (Figure 6) and large displacements (Figure 7). The force displacement plot (Figure 8) shows significant energy dissipation under design-level displacements. The energy dissipation is less under large displacements, but the loading cycles produce very stable loops (Figure 9).

[1] Asif Iqbal, University of Northern British Columbia, Canada, asif.iqbal@unbc.ca
[2] Angelo Aloisio, University of L'Aquila, Italy, angelo.aloisio1@univaq.it
[3] Massimo Fragiacomo, University of L'Aquila, Italy, massimo.fragiacomo@univaq.it

https://doi.org/10.52202/069179-0289

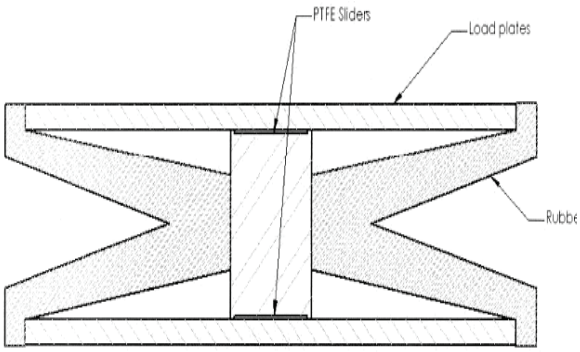

***Figure 3**: Schematic section of RoGlider*

***Figure 4**: Exterior view of RoGlider*

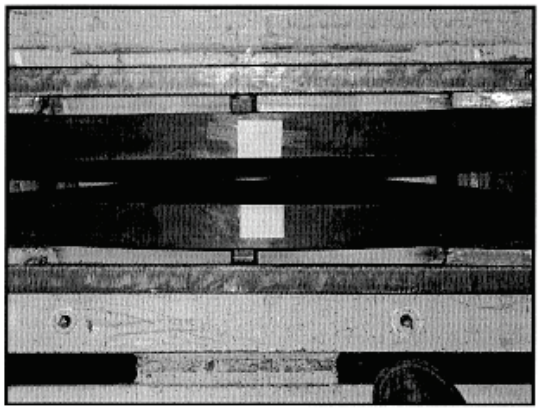

***Figure 5**: View of RoGlider with attachments during testing, under vertical load of 850 kN [1]*

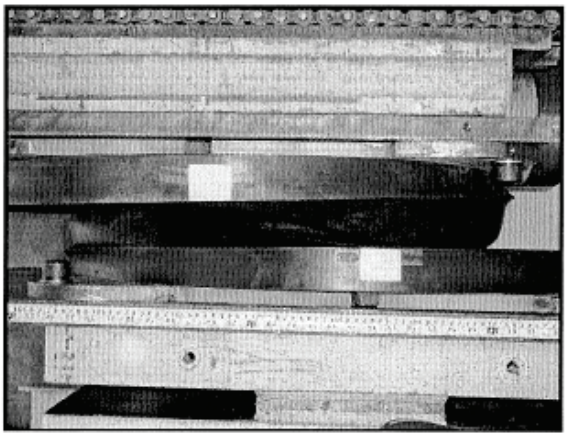

***Figure 6**: Deformed shape of RoGlider during testing, at 150 mm displacement and vertical load of 850 k N [1]*

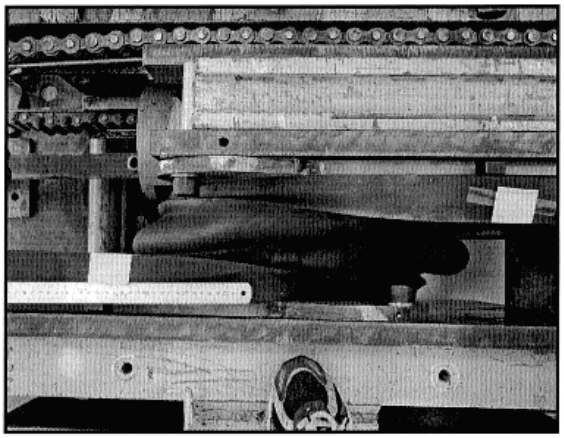

***Figure 7:** Deformed shape of RoGlider during testing, at 575 mm displacement and vertical load of 110 k N [1]*

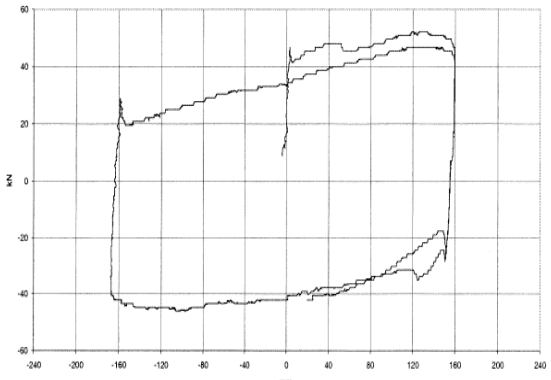

***Figure 8:** Force-displacement plot of RoGlider, under 850 kN vertical load [1]*

https://doi.org/10.52202/069179-0289

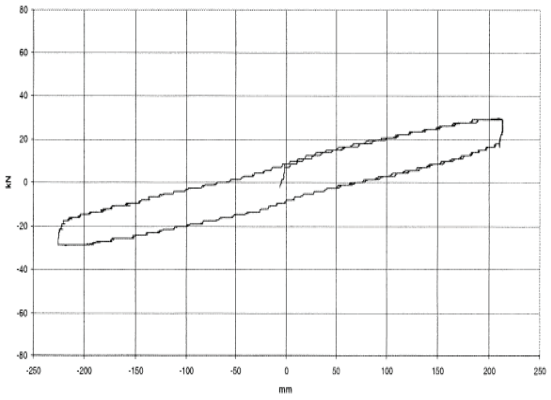

Figure 9: *Force-displacement plot of RoGlider, under 110 kN vertical load [1]*

The bearings also exhibit stable behaviour under sinusoidal loading cycles at slow (Figure 10) and high speeds (Figure 11). The coefficients of friction vary with speed (Figure 12) but the trend is consistent between slow and high speeds.

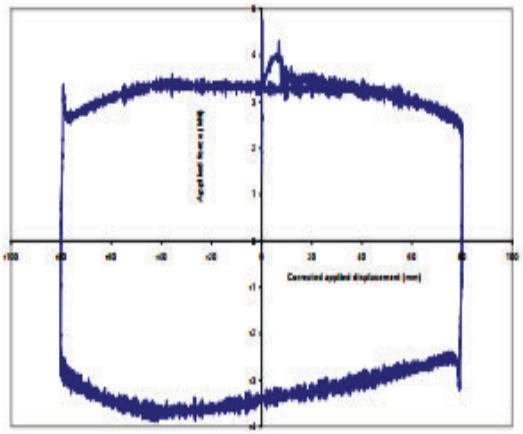

Figure 10: *Hysteresis loops of RoGlider, under sinusoidal displacement to 80 mm at 0.01 Hz [3]*

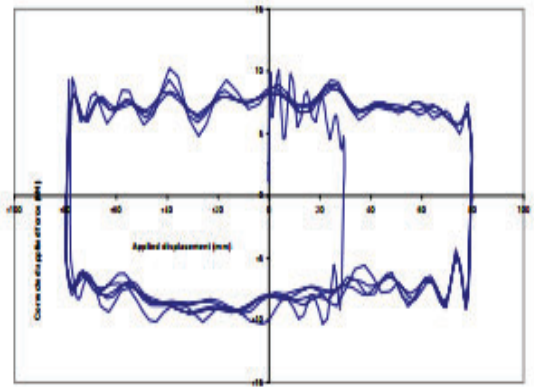

Figure 11: *Hysteresis loops of RoGlider, under sinusoidal displacement to 80 mm at 0.5 Hz [3]*

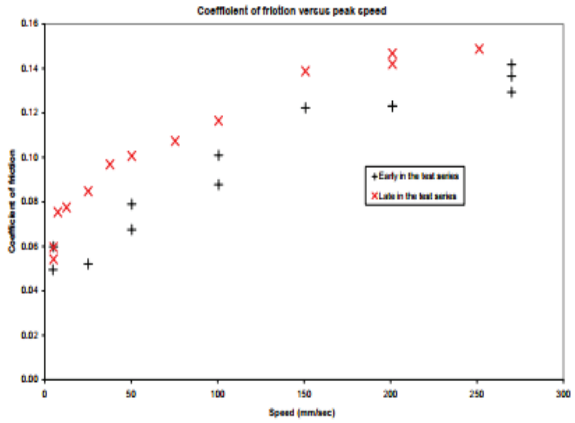

Figure 12: *Effective coefficient of friction of RoGlider [3]*

3. ROGLIDER APPLICATION

Figure 13: *Wanganui Hospital Building in New Zealand [2]*

RoGlider have been used to isolate a hospital building in Wanganui (Figure 13) in the North Island of New Zealand [2]. The bearings have been placed under the steel structure of the building (Figure 13). The load-displacement plots of the bearings used (Figure 14) again show very stable loops with significant energy dissipation capacity.

https://doi.org/10.52202/069179-0289

Figure 13: View of *Wanganui Hospital Building structure with RoGlider bearings [2]*

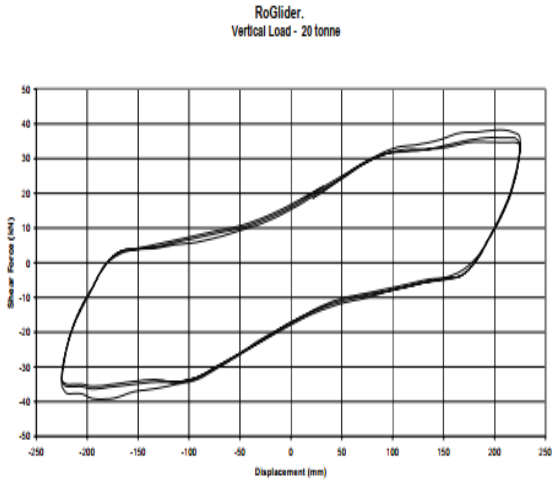

Figure 14: *Hysteresis loops of RoGlider, bearing used in Wanganui Hospital building [2]*

4. HYSTERESIS MODELLING

The authors describe the hysteresis curve of the RoGlider using a classical Bouc-Wen model. For a structural element described by a Bouc–Wen class model, the resisting force is written as

$$f_s(x, \dot{x}, z) = \alpha k_0 x + (1 - \alpha) k_0 z \qquad (1)$$

Where

fs	Resisting force
x	Displacement
x	Derivative of x with respect to time
z	Auxiliary variable representing inelasticity
α	Post- to-pre-yield stiffness ratio
k_0	Initial stiffness

The evolution of z is determined by an auxiliary ordinary differential equation, which can be written in the form

$$\dot{z} = \dot{x}[A - |z|^n \psi(x, \dot{x}, z)] \qquad (2)$$

Where

z	Derivative of z with respect to time;
A	Parameter controlling scale of hysteresis loops;
n	Sharpness parameter of hysteresis loops, n>0;
ψ	Other shape features of the hysteresis loop;

The ψ functions of the original Bouc–Wen model used in this paper is

$$\psi_{Bouc-Wen} = \gamma + \beta sgn(\dot{x}z) \qquad (3)$$

Where

$\psi_{Bouc-Wen}$ Shape parameter, $\gamma > 0$, $-\gamma < \beta < +\gamma$;

5. MODEL VALIDATION AND DETAILS

Comparison between the simulated and experimental data in terms of hysteresis curve, force-time and energy-time functions are shown in Figures 15, 16 and 17, respectively.

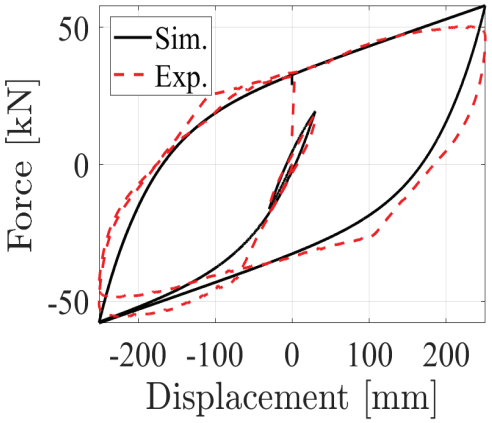

Figure 15: *Hysteresis comparison*

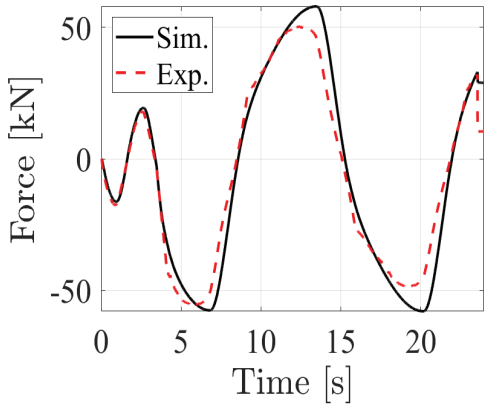

Figure 16: *Comparison of force vs. time*

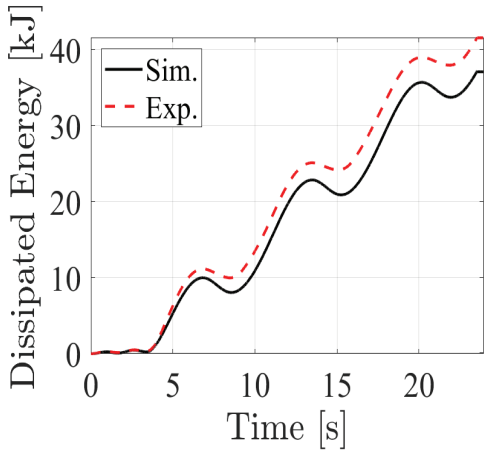

Figure 5: *Energy vs. time functions*

Hysteresis curve parameters in Figures 3, 4 and 5 estimated using Ordinary Least Square Operator [5,6] are:

Table 1: *Estimated classical Bouc-Wen model parameters*

Parameters	RoGlider
α	0.15
k_0	0.65
n	1.08
β	20.5
γ	0.1

6. RESULTS

The paper discusses the effect of variable mass on the gain spectra of a SDOF oscillator, whose restoring force is represented by the Bouc-Wen model in Figure 3. The gain spectra are defined as:

$$\mathcal{G}(T,\xi) = \frac{\max(|x_1(t)|}{\max(|x_2(t)|} \quad (4)$$

where $\mathcal{G}$ is the gain spectrum, ξ is the viscous damping ratio, $x_1(t)$ is the seismic response of a SDOF oscillator with restoring force described by the Bouc-Wen model, $x_1(t)$ seismic response of a viscoelastic SDOF system with damping ξ. If $\mathcal{G} < 1$, the use of the RoGlider is advantageous. The inelastic restoring force contributes to the equilibrium of a single-degree-of-freedom oscillator (SDOF), which is representative of the dynamic response of the RC frame. The analysis focuses on the behavior of a SDOF system neglecting all aspects related to the practical scenario of a full-size building. The equilibrium of a lumped mass above the frame yields the following ordinary differential equation (ODE) under earthquake excitation:

$$m\ddot{x} + f_t = -m\ddot{x}_g \quad (5)$$

where m is the mass equal to 20 t, x is the displacement, $\ddot{x}$ is the double derivative of x with respect to time, f_t is the resisting inelastic force, and $\ddot{x}_g$ is the ground acceleration. Fig.4 shows the comparison between the seismic response of a specific SDOF with mass equal to 20ton, under the El-Centro earthquake.

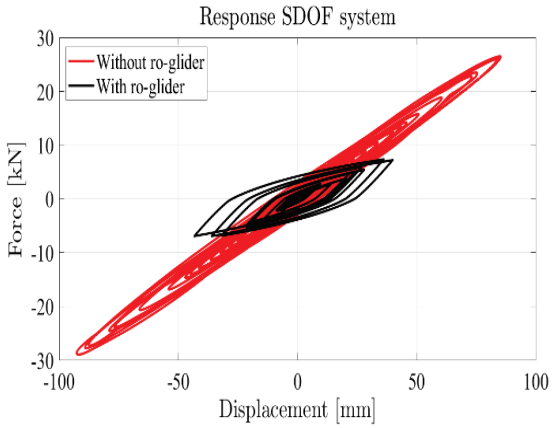

Figure 17: *Response of a SDOF system with mass M=20ton to the El Centro earthquake*

Figure 18 plots the inelastic gain spectra, defined in Eq.(4) estimated using earthquake records listed in Aloisio et al. [6].

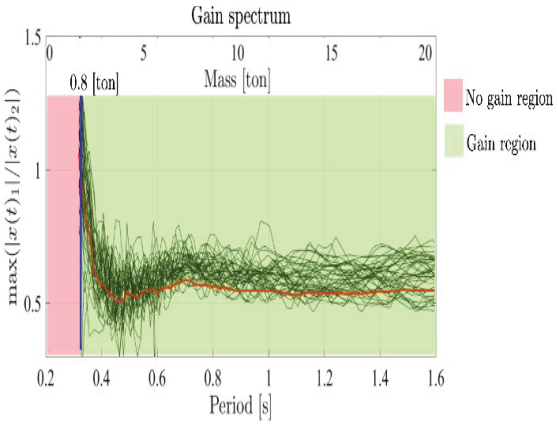

Figure 18: *Gain Spectra*

The averaged gain spectrum, in red, exhibits a peculiar shape. If the lumped mass is lower than 0.8 ton, the maximum displacement attained by the two systems with and without the Ro-glider are equal. This mass value corresponds to a natural period equal to 0.35s. There is a region of minimum between 0.4 and 0.6s, where the gain spectrum attains 0.5. For natural periods higher than 0.6s, the gain spectrum stabilizes at 0.55.

7. CONCLUSIONS

The proposed model promises to represent the isolation system with sufficient accuracy. It also demonstrates usefulness of RoGlider as a practical option for seismic design of lightweight structures. Further work on applicability and seismic performance of the system in multi-story timber buildings is currently underway.

REFERENCES

[1] Robinson, W. H., Gannon, C. R. and Meyer, J. The RoGlider – A sliding bearing with an elastic restoring force, *Bulletin of the New Zealand Society for Earthquake Engineering*, 39(1), 2006, 81-84.

[2] Robinson, W. H. and Gannon, C. R. The A seismic isolation of Wanganui hospital with RoGliders, Bulletin of the New Zealand Society for Earthquake Engineering, 41(4), 2008, 261-263.

[3] Thurston SJ. 2006. 'Base Isolation of Low Rise Light And Medium-Weight Buildings'. BRANZ *Study Report SR 156*. BRANZ Ltd, Judgeford, New Zealand.

[4] Thurston SJ. 'Base Isolation of Timber-Framed Buildings', Bulletin of the New Zealand Society for Earthquake Engineering. Vol. 40, No. 4, December 2007.

[5] Aloisio, A., Alaggio, R., Köhler, J., and Fragiacomo, M. Extension of generalized bouc-wen hysteresis

https://doi.org/10.52202/069179-0289

modeling of wood joints and structural systems. *Journal of Engineering Mechanics*, 2020, 146(3):04020001.

[6] Aloisio, A., Boggian, F., Tomasi, R., and Fragiacomo, M. (2021). Reliability-based assessment of ltf and clt shear walls under in-plane seismic loading using a modified bouc-wen hysteresis model. ASCE-ASME Journal of Risk and Uncertainty in Engineering Systems, Part A: Civil Engineering, 7(4):04021065.